Design and experimental verification of near-field Ka-band probe based on wideband OMJ with minimum higher-order spherical mode content

Foged, L. J. ; Giacomini, A.; Morbidini, R; Estrada, J.; Pivnenko, Sergey

Published in:
Proceedings of the 34th Annual Symposium of the Antenna Measurement Techniques Association

Publication date:
2012

Document Version
Publisher's PDF, also known as Version of record

DESIGN AND EXPERIMENTAL VERIFICATION OF KA-BAND NEAR FIELD PROBE BASED ON WIDEBAND OMJ WITH MINIMUM HIGHER ORDER SPHERICAL MODE CONTENT

L. J. Foged, A. Giacomini, R. Morbidini
SATIMO, Via dei Castelli Romani 59, 00040 Pomezia, Italy
Email: lfoged@satimo.com, agiacomini@satimo.com, rmorbidini@satimo.com

J. Estrada
SATIMO US, 2105 Barret Park Dr, Suite 104, Kennesaw, GA 30144 - USA
Email: jestrada@satimo.com

S. Pivnenko
Dept. of Electrical Engineering, Technical University of Denmark, Kgs. Lyngby – Denmark
Email: sp@elektro.dtu.dk

ABSTRACT

A desired feature of modern field probes is that the useable bandwidth should exceed that of the Antenna Under Test (AUT) [1]. Recent developments in probe and orthomode junctions (OMJ) technology has shown that bandwidths of up to 4:1 are achievable [2-5]. The probes are based on inverted ridge technology capable of maintaining the same high performance standards of traditional probes

However, in typical Spherical Near Field (SNF) measurement scenarios, the applicable frequency range of the single probe can also be limited by the content of $\mu \neq 1$ spherical modes in the probe pattern [6-7]. This is because the traditional NFtoFF software applies probe correction under the assumption that the probe pattern is fully specified from knowledge of the E-and H-plane patterns only [8]. While this condition is guaranteed for virtually any type of probe for small illumination angles of the AUT and/or a long probe/AUT distance this assumption may lead to unacceptable errors in special cases.

This paper describes the design and experimental verification of a Ka-band probe based on the inverted ridge technology. The probe is intended for high precision SNF measurements in special conditions that require less than -45dB higher order spherical mode content. This performance level has been accomplished through careful design of the probe and meticulous selection of the components used in the external balanced feeding scheme.

The paper reports on the electrical and mechanical design considerations and the experimental verification of the modal content.

Keywords: wideband antennas; open- ended waveguides; dual polarized antennas; antenna measurements.

1. Introduction

Dual polarized probes for modern high precision measurement systems have strict requirements in terms of pattern shape, polarization purity, return loss and port-to-port isolation. As a desired feature of modern probes the useable bandwidth should exceed that of the antenna under test so that probe mounting and alignment is performed only once during a measurement campaign [1]. Consequently, the probe design is often a trade-off between performance requirements and usable bandwidth.

Recently, a new orthomode junction (OMJ) and probe design based on inverted ridge technology has been developed capable of achieving as much as 4:1 bandwidth while maintaining the high performance standards of traditional probe designs [2-7].

Measurements and simulations performed in [6-7] show that in the inverted ridge technology probes, the fourfold symmetry support spherical modes with mode index $\mu \neq 1$. The odd spherical modes with index $\mu = 3,5,7..$ derive from the physical design of the inverted ridge structure and are basically insensitive to excitation errors. The odd modes content can therefore be limited to levels below any practical concern by a careful design of the inverted ridge layout. The even spherical modes with index $\mu = 0,2,4..$ derive mainly from the excitation errors of the balanced feeding and can therefore be controlled by a meticulous selection of the components of the external balanced feeding scheme as discussed in [6-7].

Considering a threshold of around -40dB for the power content of higher order spherical modes, similar to the mode truncation level of most reference facilities, the frequency range of an inverted ridge probe is generally better than 2:1. By careful mechanical and electrical design the desired maximum of -45dB higher order spherical modes content can be achieved.

2. Probe Specification

The probe is intended for high precision Ka-band SNF measurements. The specified bandwidth of 33-37GHz is only slightly higher than 1.1:1 and does not pose a significant design problem in terms of bandwidth. The electrical performance specification for the probe requires low directivity and high angular illumination, low loss, good return loss performance, high port-to-port isolation and excellent cross polar discrimination on-axis. The most important design parameter for the OMJ design is that the single spherical mode power content of the probe pattern, $\mu \neq 1$, must be less than -45dB. The specific electrical probe requirements are summarized in Table 1.

Item	Specification
Polarisation	Dual linear
Bandwidth	33 – 37 GHz
Return Loss	< -12 dB
Port to Port isolation	> 45 dB
Cross polar discrimination	>45 dB on axis
Polarisation orientation	< 0.3°
$\mu \neq 1$ spherical mode content	< -45dB

Table 1: Electrical probe requirements.

3. Probe Design

The SATIMO DOEW18000 open ended waveguide consists of a wideband OMJ covering the entire bandwidth from 18-40GHz. This probe can either be used as a fixed wide band probe covering the entire bandwidth or equipped with different, interchangeable apertures each designed for different antenna measurement conditions as discussed in [5]. The Ka-band probe was devised as a custom designed aperture mounted on the standard OMJ of the DOEW18000 as shown in Figure 1.

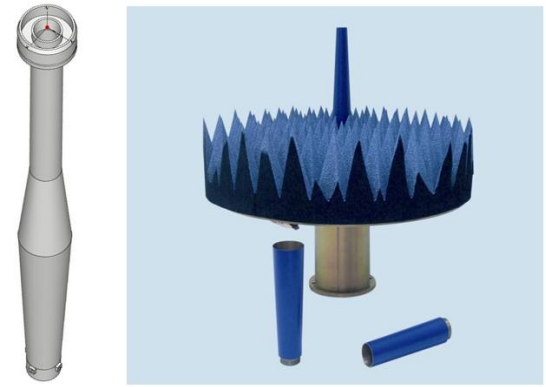

Figure 1 – Custom designed aperture (left) for the OMJ of the DOEW18000 wide band probe with interchangeable apertures (right).

The "aperture" comprises a short conical waveguide that connects the OMJ to the radiating structure of the probe. By designing a specific narrow band aperture for the existing OMJ the higher order spherical mode content can be readily controlled. As discussed in [6-7] the odd spherical modes with index $\mu=3,5,7..$ can easily be limited to levels below any practical concern by the physical layout of the aperture.

The even spherical modes with index $\mu=0,2,4..$ derive mainly from the excitation errors of the balanced feeding of the OMJ. By forcing the lower frequency of the aperture closer to the operating frequency the probe becomes less sensitive to excitation errors in the bandwidth of interest.

The effective excitation error from a given OMJ is difficult to measure accurately but upper bound can be derived from measurements on specific components. Using numerical simulation the radiation pattern of the entire probe assembly can be determined with different levels of excitation error from ideal balanced excitation. The spherical mode power spectrum versus frequency can then be determined from the spherical wave expansion of the radiation pattern.

Using this approach, the calculated spherical modal content including excitation errors up to 1dB and 8° phase error is shown in Figure 2. The actual excitation error should be far less than this value. Even with such high OMJ excitation error the even mode content of the probe stays below 90 dB in the frequency range of interest. Considering these values, the probe could safely operate in the 32-38GHz range. The odd higher order spherical modes are also well below levels of practical concern.

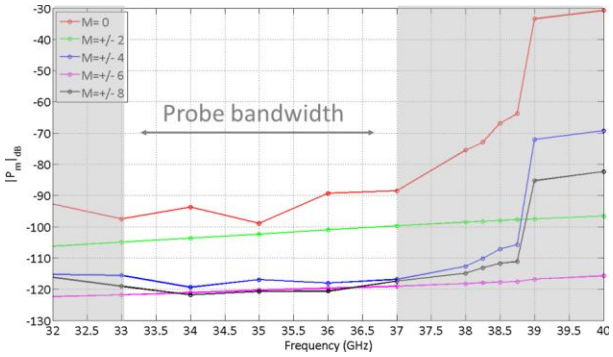

Figure 2 – Calculated spherical mode power spectrum with frequency assuming OMJ excitation errors of 1dB, 8° deviation from ideal balanced condition.

3. Experimental Performance Verification

For verification testing, the Ka-band probe was calibrated in the DTU-ESA Spherical Near-Field Antenna Test Facility at the Technical University of Denmark (DTU). The final probe mounted on the antenna positioner is shown in Figure 3.

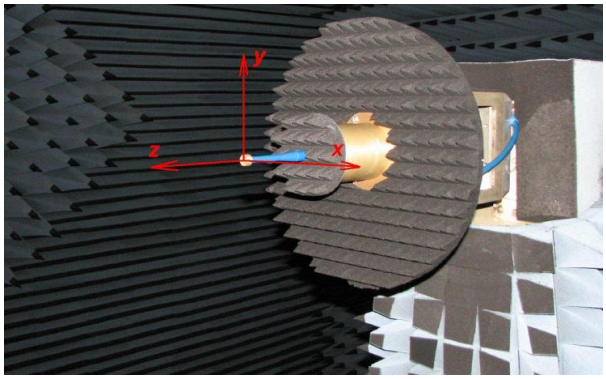

Figure 3 – Final Ka-band probe mounted on the probe tower in the DTU-ESA Facility.

The measured S-parameters for the probe are shown in Figure 4. All measured values comply with the specification.

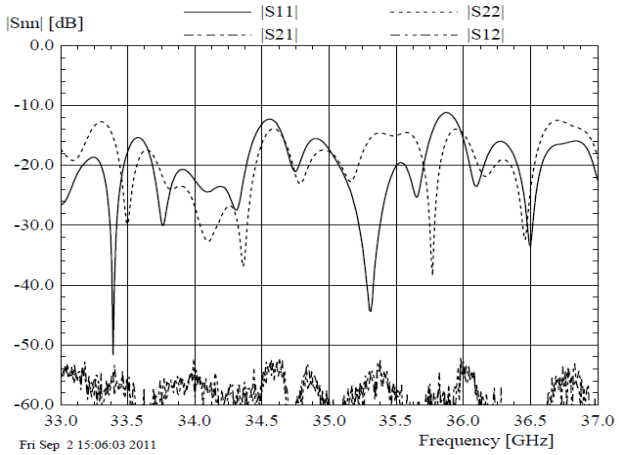

Figure 4 – Measured S-parameters of the final Ka-band probe.

The measurement of the radiation characteristics of the probe was carried out for each port separately with the unused port terminated in a 50 Ohms load. For each port, the full-sphere measurement was repeated twice, with different scanning schemes, to suppress the effect of mechanical inaccuracies in the setup, scattering effects, drift and noise. Therefore, it is considered that the effect of the mechanical sources of inaccuracy is negligible, while the effects of the scattering, drift and noise are reduced by a factor $\sqrt{2}$. From standard measurement uncertainty analysis the 3σ value for the on-axis directivity is 0.10 dB and 0.40 dB for the on-axis gain.

The on-axis polarization measurement was carried out versus the probe with known polarization characteristics. For each port of the probe, a polarization pattern was measured by rotating the probe about the horizontal axis [8]. The polarization characteristics and the amplitude phase factor (channel balance) of the probe were then determined from these measurements. The measured on-axis axial ratio and tilt angle and the probe amplitude phase factor are shown in Figure 5.

Freq. [GHz]	port X Axial Ratio [dB]	port X Tilt Angle [deg]	port Y Axial Ratio [dB]	port Y Tilt Angle [deg]
33.0	48.3	0.21	48.0	-89.79
33.1	46.0	-0.21	54.6	-89.78
33.2	56.8	0.10	64.8	-89.83
33.3	44.5	0.04	51.4	89.86
33.4	44.1	-0.22	57.5	-89.90
33.5	73.9	-0.04	52.4	89.99
33.6	52.0	0.03	61.5	-89.86
33.7	52.4	0.16	57.3	-89.75
33.8	44.4	-0.08	43.5	89.96
33.9	52.0	0.04	46.4	89.76
34.0	50.3	0.33	52.0	89.89
34.1	43.1	0.11	46.9	-89.93
34.2	65.7	-0.24	48.5	-89.80
34.3	45.3	-0.02	57.3	-89.76
34.4	51.8	-0.18	62.9	89.96
34.5	43.0	0.08	61.4	-89.85
34.6	49.3	-0.30	47.3	89.89
34.7	45.9	-0.10	59.5	89.93
34.8	53.0	0.40	51.2	-89.79
34.9	70.7	-0.22	57.7	89.93
35.0	56.7	0.06	59.2	-89.97
35.1	62.8	0.27	47.9	-89.99
35.2	43.5	-0.01	53.6	-89.93
35.3	58.7	0.09	60.1	-89.78
35.4	50.3	-0.01	56.1	-89.95
35.5	46.6	0.20	49.1	89.90
35.6	42.4	-0.11	58.0	89.94
35.7	46.5	-0.27	43.4	89.87
35.8	49.0	-0.10	43.8	89.98
35.9	49.5	0.38	48.3	-89.82
36.0	54.0	-0.02	49.5	-89.94
36.1	53.7	-0.35	44.4	89.40
36.2	46.1	0.27	47.1	-89.89
36.3	59.8	0.08	43.8	89.94
36.4	43.9	-0.06	50.4	-89.84
36.5	53.6	-0.08	54.1	89.95
36.6	57.9	0.21	47.0	89.80
36.7	43.7	0.08	48.4	-89.79
36.8	45.4	-0.28	62.1	89.93
36.9	64.1	-0.04	56.6	-89.93
37.0	45.8	0.10	46.7	89.85

Freq. [GHz]	$\mathrm{Re}(A_{x/y})$	$\mathrm{Im}(A_{x/y})$	$A_{x/y}$ [dB]	$A_{x/y}$ [deg]
33.0	-0.9780	-0.1142	-0.13	173.34
33.1	-0.9734	-0.0971	-0.19	174.30
33.2	-0.9656	-0.0723	-0.02	175.85
33.3	-1.0298	-0.1023	0.30	174.33
33.4	-1.0080	-0.1333	0.14	172.46
33.5	-0.9843	-0.1159	-0.08	173.29
33.6	-1.0004	-0.1037	0.05	174.08
33.7	-1.0036	-0.1254	0.10	172.88
33.8	-0.9762	-0.1333	-0.13	172.22
33.9	-0.9671	-0.1259	-0.22	172.59
34.0	-0.9517	-0.1132	-0.37	173.22
34.1	-0.9579	-0.0957	-0.33	174.29
34.2	-0.9633	-0.0884	-0.29	174.76
34.3	-0.9732	-0.0898	-0.20	174.73
34.4	-0.9632	-0.1061	-0.27	173.72
34.5	-0.9367	-0.0822	-0.53	174.98
34.6	-0.9639	-0.0444	-0.31	177.36
34.7	-1.0064	-0.0667	0.07	176.21
34.8	-0.9912	-0.0997	-0.03	174.26
34.9	-0.9689	-0.0982	-0.23	174.21
35.0	-0.9571	-0.0863	-0.35	174.85
35.1	-0.9540	-0.0751	-0.38	175.50
35.2	-0.9698	-0.0496	-0.26	177.07
35.3	-1.0121	-0.0547	0.12	176.91
35.4	-1.0254	-0.1028	0.26	174.28
35.5	-0.9922	-0.1228	0.00	172.95
35.6	-0.9788	-0.1259	-0.11	172.67
35.7	-0.9547	-0.1332	-0.32	172.06
35.8	-0.9078	-0.1127	-0.77	172.93
35.9	-0.9150	-0.0560	-0.76	176.50
36.0	-0.9573	-0.0380	-0.37	177.72
36.1	-0.9823	-0.0580	-0.14	176.62
36.2	-0.9763	-0.0862	-0.17	174.95
36.3	-0.9525	-0.0850	-0.39	174.90
36.4	-0.9402	-0.0642	-0.52	176.09
36.5	-0.9647	-0.0382	-0.31	177.73
36.6	-0.9880	-0.0490	-0.09	177.16
36.7	-0.9869	-0.0718	-0.09	175.84
36.8	-0.9781	-0.0764	-0.17	175.53
36.9	-0.9733	-0.0702	-0.21	175.88
37.0	-0.9783	-0.0783	-0.16	175.42

Figure 5 – Measured on-axis radiation characteristics. Axial ratio/tilt (left), amplitude phase factor (right).

The measured directivity pattern of the probe at 35GHz (center frequency) for both X and Y probe ports are shown in Figure 6.

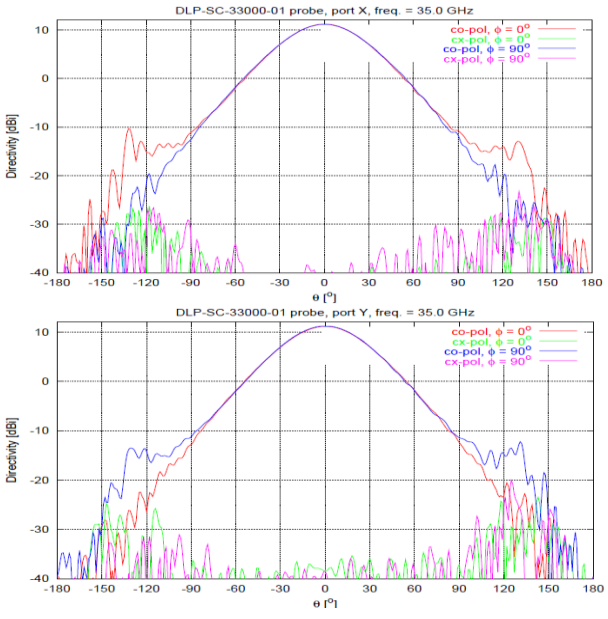

Figure 6 – Measured probe pattern @ 35GHz.

The measured probe boresight directivity for both probe ports in 41 frequency points in the 33-37GHz frequency range is shown in Figure 7.

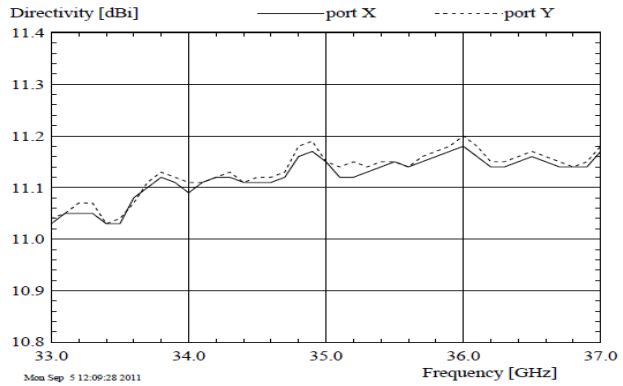

Figure 7 – Measured peak directivity in 41 frequency points in the 33-37GHz range.

The normalized μ-mode power spectrum for both ports of the probe at 35.0 GHz is shown in Fig. 8. The spectra at the other frequencies in the 33-37GHz bandwidth have very similar behavior.

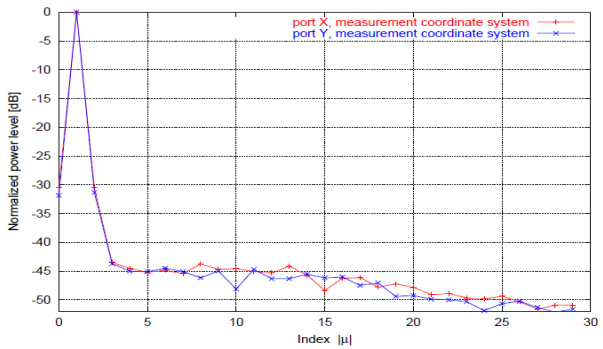

Figure 8 – The normalized μ-mode power spectrum of the probe at 35.0 GHz before translation of the reference measurement system.

It is seen from Figure 8 that the spectrum with indices $\mu > 2$ is very low, but the spectrum indices $\mu = 0$ and $\mu = 2$ are at the level of some −30dB, much higher than expected. By examining closer the measured probe patterns it was found that, while the amplitude patterns are highly symmetric, the phase pattern possesses some asymmetry. It is known that asymmetry of the phase pattern for a structurally symmetric antenna can be caused by a translated phase reference point, i.e. the origin of the measurement coordinate system.

By translating the phase reference point of the measured far-field pattern by small amounts both along x-axis and along y-axis it was possible to achieve a symmetric phase pattern in both E and H planes. This was done systematically for both probe ports at 5 frequencies within the 33-37 GHz frequency range. It was found that an average displacement by +0.10 mm along the x-axis and by +0.09 mm along the y-axis would restore the expected symmetric phase pattern for both ports in both planes and at all 5 frequencies. Both the mechanical set-up in DTU and the actual probe interface were closely examined and it was concluded that both systems have mechanical errors below these values. After further examination, this mechanical error was attributed to the mechanical interface used specifically for the measurements in the DTU range. Since the probe will be used without this interface in its final configuration it was decided to accept the translated patterns as references for the actual probe performance.

The normalized μ-mode power spectrum for both ports of the probe at 35.0 GHz after translation of the reference coordinate system along the x and y-axis , thus correcting for the pointing error is shown in Fig. 9.

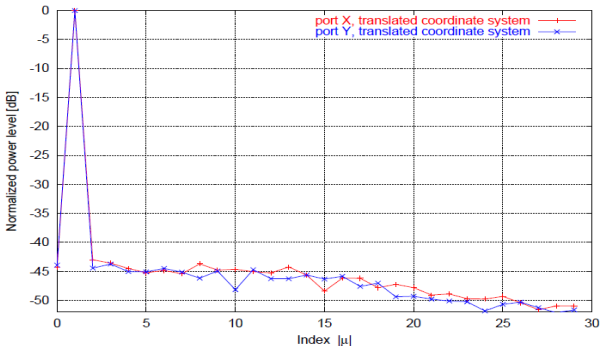

Figure 9 – The normalized μ-mode power spectrum of the probe at 35.0 GHz after translation of the reference measurement system.

As can be seen in Figure 9 all indices in the power spectrum of the probe are very close to the expected values of around -45dB.

4. Conclusion

A Ka-band probe based on the inverted ridge technology has been designed, manufactured and tested. The probe was devised as a custom designed aperture mounted on the standard OMJ of the DOEW18000. The probe is intended for high precision SNF measurements in special conditions that require less than -45dB higher order spherical mode content. This performance level has been accomplished through careful design of the probe and meticulous selection of the components used in the external balanced feeding scheme.

The probe performance has been verified in the DTU-ESA Spherical Near-Field Antenna Test Facility. The high accuracy radiation measurements revealed an alignment error of the test mechanical interface of roughly 0.14mm. Upon correction, the low level of higher order spherical modes of the probe pattern was confirmed.

5. References

[1] ANSI/IEEE Std 149-1979 “IEEE Standard Test Procedures for Antennas”

[2] L. J. Foged, A. Giacomini, L. Duchesne, C. Feat, "Wide-band dual polarized probes for near field antenna measurements" AMTA 2006, October 22-27, Austin TX.

[3] L. J. Foged, A. Giacomini, S. Pivnenko, “Wide band dual polarized probes for near and farfield measurement systems”, AMTA 2007, November 4-9, 2007 St. Louis, MO, USA.

[4] L. J. Foged, A. Giacomini, “Wide-Band Dual Polarized Probes for Near Field Antenna Measurements”, IEEE International Symposium on Antennas and Propagation 2007, June 10-15, Honolulu, HI, USA.

[5] L. J. Foged, A. Giacomini, R. Morbidini, "Wideband dual polarised open-ended waveguide probe", AMTA 2010 Symposium, October, Atlanta, Georgia, USA.

[6] L. J. Foged, A. Giacomini, R. Morbidini, “Probe performance limitation due to excitation errors in external beam forming network”, 33rd Annual Symposium of the Antenna Measurement Techniques Association, AMTA, October 2011, Englewood, Colorado, USA

[7] L. J. Foged, A. Giacomini, R. Morbidini, “ “Wideband Field Probes for Advanced Measurement Applications**”,** IEEE COMCAS 2011, 3rd International Conference on Microwaves, Communications, Antennas and Electronic Systems, Tel-Aviv, Israel, November 7-9, 2011.

[8] Hansen J. E. (ed.), “Spherical Near-Field Antenna Measurements”, Peter Peregrinus, Ltd., on behalf of IEE, London, 1988.